Reactive and Functional Polymers 108 (2016) 86–93

Contents lists available at ScienceDirect

Reactive and Functional Polymers

journal homepage: www.elsevier.com/locate/react

Dendrons with urea/malonamide linkages for gate insulators of n-channel organic thin film transistors

Yu-Yi Hsu [a], Shih-Chieh Yeh [a,b], Shih-Hsun Lin [b], Chin-Ti Chen [b,*,1], Shih-Huang Tung [a,*,1], Ru-Jong Jeng [a,*]

[a] Institute of Polymer Science and Engineering, National Taiwan University, Taipei 106, Taiwan
[b] Institute of Chemistry, Academia Sinica, Taipei 10617, Taiwan

ARTICLE INFO

Article history:
Received 25 February 2016
Received in revised form 9 May 2016
Accepted 9 May 2016
Available online 11 May 2016

Keywords:
Dendron
Gate insulator
Electron mobility
I_{on}/I_{off} ratio
GIWAXS

ABSTRACT

A series of urea/malonamide dendritic molecules were prepared as gate insulators for organic thin film transistors (OTFTs). This series of molecules with different degrees of branching possess peripheral stearyl groups are dendrons generation 0.5 (G0.5), generation 1 (G1), generation 1.5 (G1.5), generation 2 (G2) and generation 2.5 (G2.5). In addition, two types of tetracarboxylic diimide derivatives, i.e. perylene diimide (PDI) and naphthalene diimide (NDI) with two different chain lengths of fluorinated alkyl end groups were prepared as semiconductors for OTFTs such as NDI-C_4F_7, NDI-C_7F_9, PDI-C_4F_7 and PDI-C_7F_9. The n-channel types of OTFTs were fabricated by spin-coating the gate insulators on Si/SiO_2 substrates, and then depositing the semiconducting layers in vacuum without heating the substrate. Silver was used as contact electrodes for source and drain. The performance of OTFTs with dendrons as gate insulators were better than that of OTFTs modified by octadecyltrichlorosilane (ODTS). Moreover, the threshold voltages (V_{th}s) of OTFTs shifted from positive voltage to negative voltage as the device was incorporated with higher generation of dendrons. This is because of different dielectric constants or surface energies between the interface of gate insulator and semiconducting layer. Among all samples in this study, the n-channel OTFT comprising PDI-C_4F_7 and G1.5 exhibited the best performance. In addition, an enhanced electron mobility and I_{on}/I_{off} ratio measured under ambient condition were 4.71×10^{-4} cm^2 V^{-1} s^{-1} and 7.7×10^3, respectively. Apart from that, the influence of semiconducting molecular packing order on dendron gate insulator layers was investigated by grazing-incidence wide-angle X-ray scattering (GIWAXS) and atomic force microscopy (AFM). Furthermore, pentacene-based p-channel OTFTs with G1.5 gate insulator also exhibited the highest performance. These OTFTs achieved 0.1 cm^2 V^{-1} s^{-1} and 6.3×10^4 for mobility (μ) and I_{on}/I_{off} ratio, respectively.

1. Introduction

Organic thin film transistors (OTFTs) have been extensively studied for the past decade. These promising electronics have been found applicable in flexible displays, invertors, disposable sensors, etc. due to the advantages of flexibility, large area fabrication and low cost [1]. Recently, perylene diimide (PDI) [2–4] and naphthalene diimide (NDI) derivatives were utilized as n-channel materials due to the high charge mobility and air stable in ambient conditions [5–8]. However, vacuum deposited or solution processed PDI or NDI derivatives sometimes show lower electron mobility because of poor polycrystalline or granular morphologies on the substrates [9,10]. To obtain greater grain size of crystalline structure, the substrate is always heated at high temperatures to achieve superior device performance during thin film deposition. On the other hand, the stacking of semiconducting layers is also influenced by gate insulators (or gate dielectric layers). The surface properties of gate insulators would play a role in influencing the contact resistances, electron-trapping sites, grain size, molecular packing order or film morphology of the semiconductors [11–15]. Hence, some types of materials have been developed as gate insulators such as self-assembled monolayers (SAMs) [11], polymers [12] and metal-oxide layers [14]. The practice of SAM modification is most popular because of easy processing on substrates. However, the surface with SAM modification will sometimes encounter some problems such as insufficient coverage or local structural defects on a large area, which may limit further applications. Other materials for improving the performance such as cross-linked polymers [16], multilayers [17], and organic-inorganic hybrid gate dielectrics [18] were also intensively utilized to obtain large gate capacitances, low gate leakage currents, low operating voltages, etc. Moreover, some natural materials with strong secondary bonding interactions (hydrogen bonds) like silk fibroin [19] and nature protein [20] are confirmed as good candidates for gate insulators. In this study, we first adopted the dendritic type molecules with urea/malonamide linkages for OTFT gate insulators. These monodisperse dendrons are hydrogen bond-rich and capable of forming stable self-assembled structures [21]. Because of strong intermolecular interactions, this kind of dendrons were successfully utilized in the areas of nonlinear optics

* Corresponding authors.
[1] Senior authors.

http://dx.doi.org/10.1016/j.reactfunctpolym.2016.05.008
1381-5148/

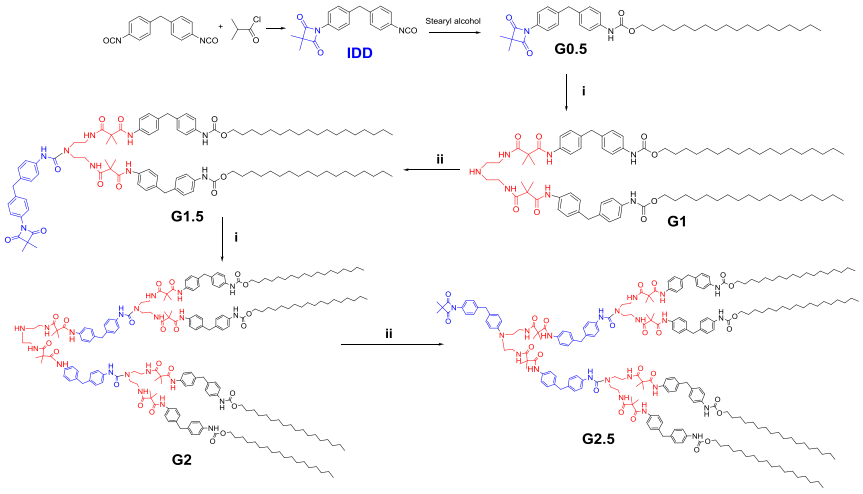

Scheme 1. Synthetic route of dendrons from bifunctional IDD to G2.5, i) diethylenetriamine (DETA) in THF, 60 °C for 6 h; ii) IDD in THF, 75 °C for 24 h.

(NLO) [22–26], shape memory materials [27,28], honeycomb structures [29,30] and ordered intercalation of montmorillonites. [31,32] Apart from that, molecules with perfluorinated alkyl (C-F) groups would exhibit strong interactions with the structures comprising long alkyl chains or carbonyl groups [33,34]. The dendrons with hydrogen bond-rich urea/malonamide linkages and peripheral long alkyl chains would certainly interact with tetracarboxylic diimide derivatives possessing perfluorinated alkyl chains on imide rings. As a result, certain properties of the semiconducting thin films will be enhanced, such as grain size and molecular packing order. The effect of gate insulators based on the dendrons will be evaluated by OTFTs performance. Moreover, the molecule packing order of the semiconducting layers investigated by grazing-incidence wide-angle X-ray scattering (GIWAXS) and atomic force microscopy (AFM) will be also discussed.

2. Experimental

2.1. Materials

Stearyl alcohol, isobutyryl chloride, methylene di-*p*-phenyl diisocyanate (MDI), triethylamine (TEA), diethylenetriamine (DETA), cyclohexane, methanol, tetrahydrofuran (THF), xylene, sulfuric acid, and hydrogen peroxide were purchased from Aldrich, Acros, and SHOWA. Octadecyltrichlorosilane (ODTS), imidazole, 2,2,3,3,4,4,4-heptafluorobutan-1-amine, 4,4,5,5,6,6,7,7,7-nonafluoroheptan-1-amine, 1,4,5,8-naphthalenetetracarboxylic dianhydride and perylene-3,4,9,10-tetracarboxylic dianhydride were purchased from Aldrich. Pentacene was purchased from Lumtec.

2.2. Synthesis

2.2.1. Dendrons with urea/malonamide linkage for gate insulator

The dendrons of different generations (from generation 0.5 (G0.5) to generation 2.5 (G2.5)) with peripheral stearyl groups were prepared via a convergent approach based on a building block, 4-isocyanato-4-(3,3-dimethyl-2,4-dioxo-acetidino)diphenyl methane (IDD) was described in previous reports [22–24,26,28,35,36], and the synthetic route are shown in Scheme 1. ^{1}H NMR profiles, FT-IR spectra and thermal properties are also shown in Supporting information.

2.2.2. Semiconducting materials: perylene and naphthalene diimide with fluoroalkyl chains

Semiconducting materials NDI-C_4F_7, NDI-C_7F_9, PDI-C_4F_7 and PDI-C_7F_9 were synthesized according to literature procedures (Scheme 2) [3,31].

2.2.2.1. General procedure for synthesis of NDI-C_4F_7: 1,4,5,8-Naphthalene-tetracarboxylicdianhydride (0.56 g, 2.094 mmol) reacted with 2,2,3,3,4,4,4-heptafluorobutan-1-amine (1.0 g, 5.025 mmol) and imidazole (8.55 g, 126 mmol) in toluene at 140 °C for 24 h. After cooling the mixture to room temperature, 2 N HCl was added and stirred for 2 h and the precipitate solid was filtrated and washed with water. After drying, the pink powder yield was 90% (1.19 g, 1.90 mmol). ^{1}H NMR ($CDCl_3$, 300 MHz): δ 8.86 (s, 4H), 5.01 (t, J = 6.3 Hz, 4H); ^{1}C NMR ($CDCl_3$, 75 MHz): δ 162.2, 131.8, 127.0, 126.3, 38.6 (t, J = 21.0 Hz); ^{1}F NMR ($CFCl_3$, 300 MHz): δ −80.2 (t, J = 12.0 Hz, 3F),

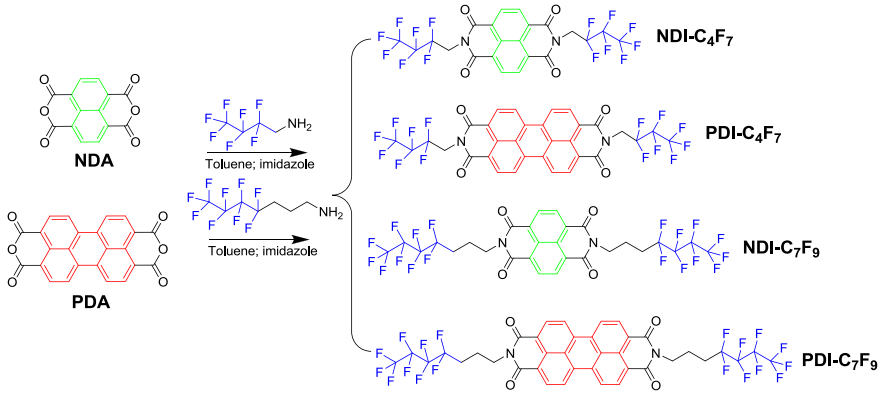

Scheme 2. Synthetic route of semiconductors NDI-C_4F_7, NDI-C_7F_9, PDI-C_4F_7 and PDI-C_7F_9.

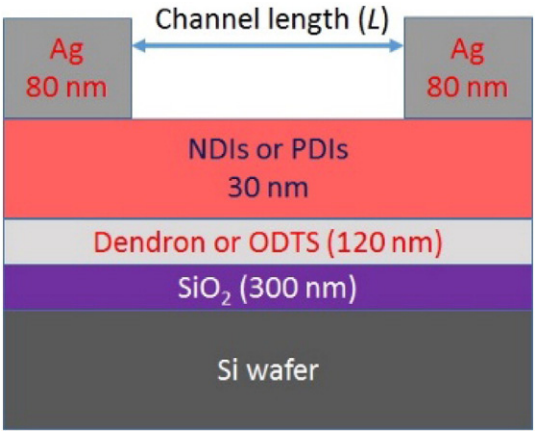

Fig. 1. Cross-section view of an OTFT device structure.

−115.7 (m, 2F), −127.5 (q, J = 15.0 Hz, 2F); FAB-MS calcd for $C_{22}H_8F_{14}N_2O_4$ 630.0 *m/z*, found $(M + H)^+$.

2.2.2.2. NDI-C_7F_9: The pink powder yield was 92%. ^{1}H NMR ($CDCl_3$, 300 MHz): δ 8.78 (s, 4H), 4.29 (t, J = 7.2 Hz, 4H), 2.27–2.08 (m, 8H); ^{1}C NMR ($CDCl_3$, 75 MHz): δ 162.7, 131.2, 126.6, 126.5, 39.9, 28.5 (t, J = 22.5 Hz), 19.6; ^{1}F NMR ($CFCl_3$, 300 MHz): δ −80.4 (t, J = 9.0 Hz, 3F), −114.2 (q, J = 12.0 Hz, 2F), −124.1 (s, 2F), −125.8 (m, 2F); FAB-MS calcd for $C_{28}H_{16}F_{18}N_2O_4$ 786.1 *m/z*, found 787.1 $(M + H)^+$.

2.2.2.3. PDI-C_4F_7: The red powder yield was 94%. ^{1}H NMR ($CDCl_3$, 300 MHz): δ 8.77 (d, J = 8.1 Hz, 4H), 8.70 (d, J = 7.8 Hz, 4H), 5.03 (t, J = 14.7 Hz, 4H); ^{1}F NMR ($CFCl_3$, 300 MHz): δ −80.2 (s, 3F), −115.7 (s, 2F), −127.5 (s, 2F); FAB-MS calcd for $C_{32}H_{12}F_{14}N_2O_4$ 754.1 *m/z*, found 755.0 $(M + H)^+$.

2.2.2.4. PDI-C_7F_9: The red powder yield was 90%. ^{1}H NMR ($CDCl_3$, 300 MHz): δ 8.70 (d, J = 8.1 Hz, 4H), 8.64 (d, J = 8.1 Hz, 4H), 4.30 (t, J = 14.7 Hz, 4H), 2.26–2.08 (m, 8H); ^{1}F NMR ($CFCl_3$, 300 MHz): δ −80.8 (s, 3F), −114.2 (s, 2F), −124.1 (s, 2F), −125.8 (s, 2F); FAB-MS calcd for $C_{38}H_{20}F_{18}N_2O_4$ 910.1 *m/z*, found 911.1 $(M + H)^+$.

2.2.3. General method

Nuclear magnetic resonance (NMR) spectra were detected by Bruker Ultra Shield 300 MHz, and mass spectroscopies were detected by JMS-700 double focusing mass spectrometer (JEOL, Tokyo, Japan). Contact angles were measured by FTA125 contact angle system. The film thickness was determined by VEECO alpha step profilometer. Morphologies of the NDI and PDI derivatives were analyzed by AFM using a VEECO DICP-II instrument operated in tapping mode at ambient temperature; the etched Si probe exhibited a resonant frequency of 131 kHz and a spring constant of 11 $N \cdot m^{-1}$. Grazing-incidence wide-angle X-ray scattering (GIWAXS) measurements were made on a beamline BL23A1 in the National Synchrotron Radiation Research Center (NSRRC). An X-ray wavelength of 0.827 Å was used and the incident angle was 0.2°. Dielectric constants of dendrons with different generations were measured by RF Impedance/Material Analyzer (E4991A). The samples were prepared by pressing the material into a slice by the oil presser, and tested from 1 MHz to 3 GHz.

2.2.4. Device fabrication and characterization

The bottom-gate top-contact (BGTC) structure of OTFTs were fabricated for characterization. Heavily n-doped silicon wafers with 300 nm thermally grown silicon dioxide were used as substrates which were cleaned by soaking in piranha solution (a mixture of 98% sulfuric acid and 30% hydrogen peroxide with volume ratio 3:1) for 2 h, then rinsed with deionized water, acetone, and isopropyl alcohol, respectively.

The SAM modified Si/SiO_2 substrates were dipped into ODTS solution (40 μL in 50 mL toluene) for 5 min. The dendron gate insulators

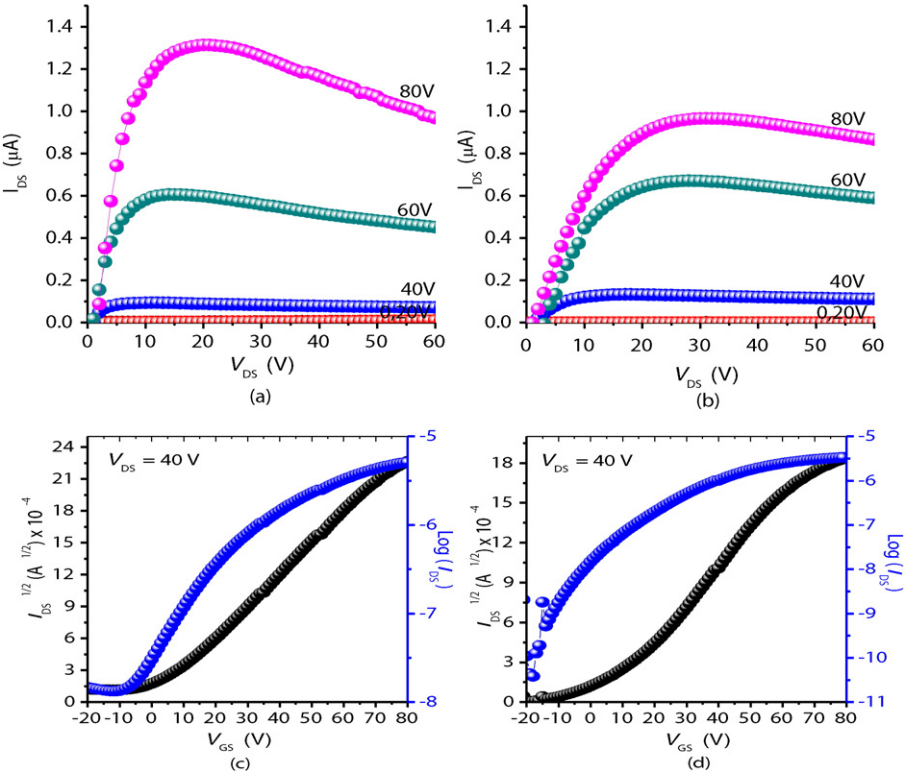

Fig. 2. OTFTs performance for ODTS as gate insulator: (a) I_{DS} vs V_{DS} of NDI-C_7F_9, (b) I_{DS} vs V_{DS} of PDI-C_4F_7, (c) $I_{DS}^{1/2}$ vs V_{GS}, Log (I_{DS}) vs V_{GS} of NDI-C_7F_9, (d) $I_{DS}^{1/2}$ vs V_{GS}, Log (I_{DS}) vs V_{GS} of PDI-C_4F_7.

Table 1
OTFT parameters[a] of four diimides with fluorinated alkyl chains (ODTS as gate insulator).

Compound	μ ($cm^2 V^{-1} s^{-1}$)	I_{on}/I_{off}	V_{th} (V)
NDI-C_4F_7	–	–	–
PDI-C_4F_7	1.64×10^{-4}	1.10×10^5	6
NDI-C_7F_9	1.50×10^{-4}	3.40×10^2	5
PDI-C_7F_9	–	–	–

[a] The mobilities were determined in the saturation regime from the slope of plots of $(I_{DS})^{1/2}$ vs V_{GS}. The *I-V* measurement were carried out under ambient condition.

were spin-coated dendron solution (10 mg/mL in chloroform) on Si/SiO_2 substrates at 1500 rpm for 30 s. The thicknesses of dendrons were around 120 nm. The NDI, PDI or pentacene semiconductor layers were vacuum-deposited with a thickness of 30 nm at rate of 0.3 Å s^{-1} under the pressure around 10^{-6} Torr. Finally, 80 nm silver was thermally evaporated onto the NDI, PDI or pentacene semiconductor layer as source and drain electrodes. The OTFT channel width (W) and channel length (L) were 2000 μm and 50 μm, respectively.

The parameters of OTFTs such as drain-source current (I_{DS}), gate voltage (V_G), mobility (μ), on–off current ratio (I_{on}/I_{off}), and the threshold voltage (V_{th}) were obtained by using Keithley Model 2400 digital multimeters with labview program under ambient condition. In all cases, 5–10 devices were measured for each dendron as gate insulators.

3. Results and discussion

3.1. OTFT measurements

Bottom-gate/top-contact (BGTC) configuration of n-channel OTFTs is shown in Fig. 1. An OTFT device consists of gate insulator and diimide semiconductor layer was prepared on a n-doped Si substrate with a 300 nm thickness of SiO_2 as dielectric layer (capacitance C_i = 10 nF cm^{-2})

The ODTS treated substrates were used as reference device as described in Experimental section. Four semiconductors such as NDI-C_4F_7, PDI-C_4F_7, NDI-C_7F_9 and PDI-C_7F_9 were synthesized for investigating the OTFTs properties. Thin films of 30 nm were vacuum-deposited on ODTS substrates without heating. Subsequently the source-drain electrodes were deposited on the top of semiconducting layer through shadow mask. The channel width (W) was 2000 μm and channel length (L) was 50 μm ($W/L = 40$). For n-channel operation mode, a positive gate voltage (V_G) was applied to cause the accumulation of electrons, and then current flows would be detected in the channel between drain and source. The mobility (μ) and threshold voltage (V_{th}) of OTFTs were determined at saturation regime from the slope of plots of drain-source current $(I_{DS})^{1/2}$ vs gate-source voltage (V_{GS}), and calculated from equation: $I_{DS} = (\mu W C_i / 2L)(V_{GS} - V_{th})^2$ .....Eq. (1). The on/off ratio (I_{on}/I_{off}) was extracted from the plot of Log (I_{DS}) vs (V_{GS}). For the ODTS modified dielectric OTFTs, I_{DS} vs V_{DS} curves at different V_{GS} values measured under ambient condition are shown in Fig. 2, with the parameters summarized in Table 1.

The mobilities of OTFTs with ODTS-modified surfaces were 1.64×10^{-4} $cm^2 V^{-1} s^{-1}$ and 1.50×10^{-4} $cm^2 V^{-1} s^{-1}$ for PDI-C_4F_7 and NDI-C_7F_9, respectively. However, NDI-C_4F_7 and PDI-C_7F_9 did not exhibit any field effect property. AFM topography images (10×10 μm^2) are shown in Fig. 3. The crystalline grains of PDI-C_4F_7 were densely packed with sizes mostly greater than 50 nm (Fig. 3b). For NDI-C_7F_9, rod shape crystals were observed (Fig. 3c). The OTFT based on PDI-C_4F_7 exhibited better mobility, 1.64×10^{-4} $cm^2 V^{-1} s^{-1}$ and larger I_{on}/I_{off} ratio up to 1.1×10^5 as respectively compared with 3.40×10^2 $cm^2 V^{-1} s^{-1}$ and 3.40×10^2 for the OTFT based on NDI-C_7F_9. No significant granular shape morphology was observed in Fig. 3a and d. The loosely packed crystal grains of NDI-C_4F_7 and PDI-C_7F_9 were too small to afford charge transporting property. This implies that it is necessary for NDI or PDI core to attach with optimized fluorinated alkyl chain lengths to achieve favorable molecular packing order on the ODTS surface. NDI-C_4F_7 with a small rigid NDI core and a short fluorinated alkyl chain made it difficult to align in an orderly fashion during vacuum deposition [3]. On the other hand, PDI-C_7F_9 with a large rigid core and a long fluorinated alkyl chain was not favorable for orderly molecular alignment either, due to the interference of the long fluorinated alkyl chain during the stacking of PDI cores [3]. Moreover, no significant V_{th} shift for these two semiconductors indicates that the effects of ODTS on NDI-C_4F_7 and PDI-C_7F_9 are similar.

Based on the above, PDI-C_4F_7 was chosen as the semiconductor to investigate the influence of dendron gate insulators. Dendrons with different degrees of branching and peripheral stearyl chains were G0.5, G1, G1.5, G2, and G2.5 (Scheme 1). These dendrons were respectively deposited on Si/SiO_2 substrates by spin-coating with a thickness of 120 nm. According to the literature [15], the performance (V_{th}) is dependent on the property of capacitance when the insulator material possesses certain functional groups. Dielectric and surface properties of these thin films are listed in Table 2. Intrinsic capacitance of these dendrons are about 22–24 nF cm^{-2}. The combined capacitance (C_i) for each dendron and SiO_2 as gate dielectric was approximately 7 nF cm^{-2} calculated by $1/C_i = 1/C_{SiO_2} + 1/C_{dendron}$ .....Eq. (2). This value is smaller than 10 nF cm^{-2} for SiO_2 single layer [3]. This indicates the capacitance properties of gate insulating layer was somewhat influenced by the presence of dendrons with urea/malonamide linkages.

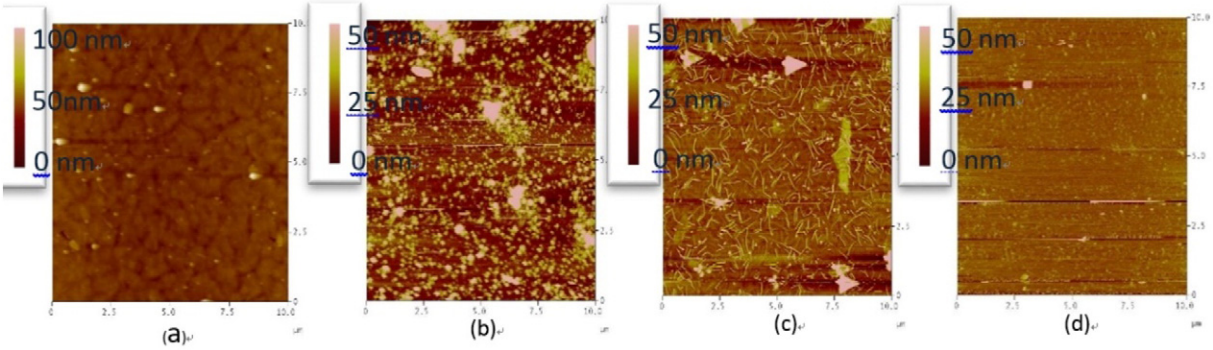

Fig. 3. AFM images of ODTS modified OTFTs: (a) NDI-C_4F_7, (b) PDI-C_4F_7, (c) NDI-C_7F_9, (d) PDI-C_7F_9. (scan area: 10×10 μm^2).

Table 2
Intrinsic properties of dendrons of different generations, and the capacitances calculated from Eq. (3).

Dendrons	Dielectric constant[a]	Capacitance (C_i)[b] (nF cm^{-2})	Total capacitance[c] (nF cm^{-2})	Surface energy[d] (mN·m^{-1})
ODTS	–	10	10	16.68
G0.5	2.49	22	6.8	17.79
G1	2.72	24	7.0	32.02
G1.5	2.73	24	7.0	30.14
G2	2.50	22	6.8	34.99
G2.5	2.64	22	6.8	33.89

[a] The values were obtained under 100 MHz.
[b] Intrinsic capacitance of dendrons. The capacitances of dendrons were obtained by $C = \varepsilon_0\varepsilon_r A/d$ .....Eq. (3). Where A is the area of electrodes, d is the thickness of dielectric layer, ε_0 is the vacuum permittivity, and ε_r is the dielectric constant, respectively.
[c] Total capacitance were obtained by $1/C_i = 1/C_{SiO_2} + 1/C_{dendron}$.
[d] Calculated from contact angle measurement.

Apart from that, the surface energies of gate insulators were also estimated (Table 2). The surface energies of dendrons were in the range of 17–35 mN·m^{-1}, which were larger than that of ODTS (16.68 mN·m^{-1}). The dendrons with higher degree of branching exhibited higher surface energies. This is due to the presence of more urea/malonamide linkages would exert more influence on the surface properties.

The parameters of OTFTs fabricated by PDI-C_4F_7 with each dendron as gate insulator layer are listed in Table 3. The plots of I_{DS} vs V_{DS} with different V_{GS} are shown in Fig. 4, whereas Fig. 5 comprises the curves of $(I_{DS})^{1/2}$ vs V_{GS} and Log (I_{DS}) vs V_{GS}. The interaction between semiconductors and dendrons was first investigated by the behavior of field effect devices. The mobilities of PDI-C_4F_7 OTFTs were 1.08×10^{-4} cm^2 V^{-1} s^{-1}, 1.13×10^{-4} cm^2 V^{-1} s^{-1}, 4.71×10^{-4} cm^{2}V^{-1}s^{-1}, 1.85×10^{-4}, 1.47×10^{-4} cm^2 V^{-1} s^{-1} for G0.5, G1, G1.5, G2, G2.5, respectively.

For G0.5, the molecule is linear with an azitidine-2,4-dione group and a long alkyl chain on both ends. Despite the absence of urea/malonamide linkage in G0.5, the OTFT with G0.5 as gate insulator was able to exhibit field effect. In Fig. 4, the I_{DS} current was increased with increasing V_{GS} for G0.5 based and ODTS based samples. It is important to note that the increase in I_{DS} is rather larger for G0.5 based sample. This is because the peripheral stearyl chain in G0.5 is similar to that in ODTS. This would assist the ordered arrangement of semiconductor PDI-C_4F_7. Fig. 5 shows similar slope values of $I_{DS}^{1/2}$ vs V_{GS} curves for G0.5 based and ODTS based OTFTs. However, the mobility of G0.5 based sample was 1.08×10^{-4} cm^2 V^{-1} s^{-1} which is smaller than that of ODTS based sample. This is due to the fact that the V_{th} was shifted to 22 V. Azitidine-2,4-dione and urethane group in G0.5 might play a role within the gate insulator to influence the charge accumulation behavior. The I_{DS} currents enhancements were also observed for PDI-C_4F_7 with dendron gate insulators such as G1, G1.5, G2 and G2.5 (Fig. 4). Unlike G0.5, the chemical structures for higher generation of dendrons possess different degrees of branching and urea/malonamide linkages that make stronger interactions with ordered PDI-C_4F_7 molecules. Among all the samples, G1.5 based device exhibited the highest mobility, 4.71×10^{-4} cm^2 V^{-1} s^{-1} with an I_{on}/I_{off} ratio of 7.7×10^3 (Fig. 5d). The best performance of OTFTs was achieved based on PDI-C_4F_7 with G1.5, but not with higher generation of dendron such as G2.5. This may possibly be caused by difficult molecular packing due to its highly branched nature as the generation of dendron further increases [28, 35]. More ordered arrangement of G1.5 would induce more charge accumulation on the surface of insulator. As a result, higher current passed through the source and drain. Furthermore, pentacene-based p-channel OTFTs with G1.5 gate insulator also exhibited the highest performance. These OTFTs achieved 0.1 cm^2 V^{-1} s^{-1} and 6.3×10^4 for mobility (μ) and I_{on}/I_{off} ratio, respectively. (Figs. S6, S7 and Table S1).

For the sake of comparison, the mobility and V_{th} for each dendron and ODTS based OTFTs are shown in Fig. 6. The mobility of OTFT based on G1.5 is 3 times as large as that of OTFT based on ODTS. This implies that G1.5 is an effective gate insulator layer to afford regular molecular packing order and larger crystal grain sizes. On the other hand, a significant V_{th} shift was also observed for the OTFT devices based on dendrons, especially for G1, G1.5, G2 and G2.5 as gate insulators. The evaluated V_{th}s for each sample were 26 V (G1), −30 V (G1.5), −40 V (G2), and −63 V (G2.5). The V_{th}s values were shifted to the range of negative voltage further for the device with higher generation of dendrons. The most negative V_{th} was found for the sample based on G2.5. Two factors for this phenomenon of V_{th} shift were summarized in literature [37–41] such as (1). certain reaction occurring at the interface of semiconductor and insulator (2). change of the dipolar environment in the insulators. These occurred reactions at interface and dipolar changes inside the gate insulators result in the formation of space-charge regions or traps that induce V_{th} change. Hydrogen bond-rich urea/malonamide linkages, reactive sites like secondary amines on the focal points of G1 and G2, or azetidine-2,4-dione on the focal points of G0.5, G1.5 and G2.5 might be possibly responsible for the V_{th} shifts of OTFTs in this study. For further investigation, the mobilities of these p-channel OTFTs were in the range of 0.05–0.1 cm^2 V^{-1} s^{-1} along with an I_{on}/I_{off} ratio up to 10^4 when the semiconductor was replaced by pentacene. No significant V_{th} shift was observed for each dendron such as G0.5, G1, G1.5, G2, and G2.5. The values of V_{th} were in the range of −4 to −11 V. Unlike NDI or PDI semiconductors with carbonyl groups on imide rings, the pentacene comprising five-fused benzene ring with no specific functional group would scarcely interact with dendron gate insulators. This further corroborates that the OTFT performance is strongly influenced by molecular interactions between semiconductors and gate insulators.

To further understand the molecular orientation of PDI-C_4F_7 deposited on dendron gate insulators, GIWAXS analysis was performed [42, 43]. 2-D GIWAXS patterns of PDI-C_4F_7 on dendron gate insulators, G0.5, G1.5, and G2.5 are shown in Fig. 7. As shown in Fig. 7a, broad diffraction pattern indicates the packing of PDI-C_4F_7 is less ordered and the crystallites are not regularly arranged on the film of G0.5. Consequently,

Table 3
Parameters of OTFTs based on PDI-C_4F_7 with different gate insulators.

Compound	μ (cm^2 V^{-1} s^{-1})	I_{on}/I_{off}	V_{th} (V)
ODTS	1.64×10^{-4}	1.1×10^5	6
G0.5	1.08×10^{-4}	1.2×10^4	22
G1	1.13×10^{-4}	1.7×10^3	26
G1.5	4.71×10^{-4}	7.7×10^3	−30
G2	1.85×10^{-4}	1.1×10^3	−40
G2.5	1.47×10^{-4}	1.1×10^2	−63

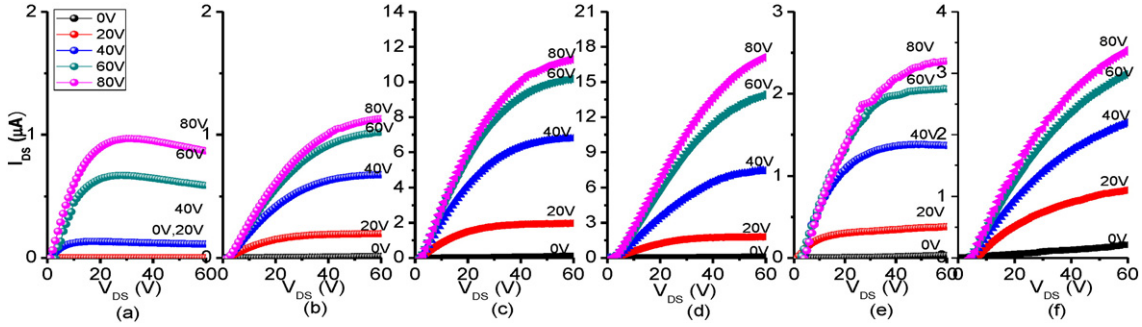

Fig. 4. *I-V* characteristics of OTFTs based on PTCDI-C_4F_7 with different gate insulators: (a) ODTS, (b) G0.5, (c) G1, (d) G1.5, (e) G2, (f) G2.5.

a relatively poor transistor behavior was obtained for the sample based on G0.5. In contrast, apparent spot-like diffraction patterns of PDI-C_4F_7 deposited on the film of G1.5 (Fig. 7b) and the film of G2.5 (Fig. 7c) indicate that the PDI-C_4F_7 molecules are highly oriented. The values of d-spacings were calculated from the diffraction peak along q_z and q_{xy} axes of the GIWAXS patterns. PDI-C_4F_7 molecular arrangements on the respective films of G1.5 and G2.5 are end-on manner, which leads to high charge transporting properties (large $I_{DS}^{1/2}$ vs V_{GS} slope) in Fig. 6d and f. While the edge-on orientation of PDI-C_4F_7 on G0.5 causes relatively lower mobility (Fig. 6b). For PDI-C_4F_7 on G1.5 dendron gate insulator, more diffraction signals are appeared at 002 and 010. This means higher order of PDI-C_4F_7 molecules on G1.5 in the q_z and q_{xy} directions. It is important to note that higher order of PDI-C_4F_7 molecules on G2.5 is only in the q_z direction. Through GIWAXS analysis, one is able to further probe molecular packing order of PDI-C_4F_7 on dendron gate insulators. It was found that G1.5 as gate insulator is most effective in inducing ordered molecular packing of semiconducting material, PDI-C_4F_7, leading to better OTFT performance. For achieving high carrier mobility, this is a feasible way to obtain better morphology for semiconductors [44–47].

4. Conclusion

Dendron gate insulators with hydrogen bond-rich urea/malonamide linkages and peripheral long alkyl chains for n-channel OTFTs comprising PDI or NDI semiconductors were first observed in this work. The device based on PDI-C_4F_7 with G1.5 gate insulator exhibited the best electron mobility, 4.71×10^{-4} cm^2 V^{-1} s^{-1} with a I_{on}/I_{off} current ratio of 7.7×10^3. Strong interactions at the interface of semiconductor and gate insulator brought about end-on ordered molecular packing as investigated by GIWAXS analysis. However, the V_{th}s values were shifted to the range of negative voltage for the devices with dendrons as gate insulators. The shift was increased as the device was incorporated with the dendrons of higher generation. NDI or PDI semiconductors with carbonyl groups on imide rings would strongly interact with urea/malonamide dendrons. On the other hand, the pentacene comprising five-fused benzene ring with no specific functional group would scarcely interact with dendron gate insulators. This provides an insight that the V_{th} shift of OTFTs could be tailored by incorporating different kinds or sizes of dendrons. This feature of controlling V_{th} is potentially useful for fabricating inverter devices [40].

Acknowledgement

The authors would like to thank Ministry of Science and Technology (MOST 103-2221-E-002-277-MY2), Taiwan for financial support.

Appendix A. Supplementary data

Supplementary data to this article can be found online at http://dx.doi.org/10.1016/j.reactfunctpolym.2016.05.008.

References

[1] D. Elkington, N. Cooling, W. Belcher, P.C. Dastoor, X. Zhou, Organic thin-film transistor (OTFT)-based sensors, Electronics 3 (2014) 234–254.
[2] B.A. Jones, A. Facchetti, M.R. Wasielewski, T.J. Marks, Tuning orbital energetics in arylene diimide semiconductors, materials design for ambient stability of n-type charge transport, J. Am. Chem. Soc. 129 (2007) 15259–15278.
[3] R.D. Schmidt, J.H. Oh, Y.S. Sun, M. Deppisch, A.M. Krause, K. Radacki, H. Braunschweig, P.M. Könemann, Z.B. Erk, High-performance air-stable n-channel organic thin film transistors based on halogenated perylene bisimide semiconductors, J. Am. Chem. Soc. 131 (2009) 6215–6228.
[4] M.C.R. Delgado, E.G. Kim, D.A. da Silva Filho, J.L. Bredas, Tuning the charge-transport parameters of perylene diimide single crystals via end and/or core functionalization: a density functional theory investigation, J. Am. Chem. Soc. 132 (2010) 3375–3387.
[5] J.H. Oh, S.L. Suraru, W.Y. Lee, M. Könemann, H.W. Höffken, C. Röger, R. Schmidt, Y. Chung, W.C. Chen, F. Würthner, Z. Bao, High-performance air-stable n-type organic transistors based on core-chlorinated napthalene tetracarboxylic diimides, Adv. Funct. Mater. 20 (2010) 2148–2156.
[6] F. Wurthner, M. Stolte, Naphthalene and perylene diimides for organic transistors, Chem. Commun. 47 (2011) 5109–5115.
[7] M. Stolte, M. Gsanger, R. Hofmockel, S.L. Suraru, F. Wurthner, Improved ambient operation of n-channel organic transistors of solution-sheared naphthalene diimide under bias stress, Phys. Chem. Chem. Phys. 14 (2012) 14181–14185.
[8] L. Li, Q. Tang, H. Li, X. Yang, W. Hu, Y. Song, Z. Shuai, Y.W. Xu, D.Z. Liu, An ultran closely π-stacked organic semiconductor for high performance field-effect transistors, Adv. Mater. 19 (2007) 2613–2617.

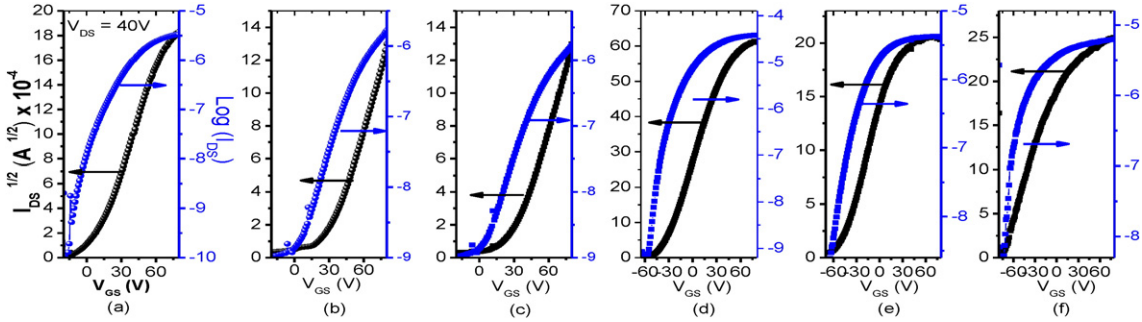

Fig. 5. Plots of $I_{DS}^{1/2}$ vs V_{GS} and Log (I_{DS}) vs V_{GS} of OTFTs based on PTCDI-C_4F_7 with different gate insulators: (a) ODTS (b) G0.5, (c) G1, (d) G1.5, (e) G2, (f) G2.5.

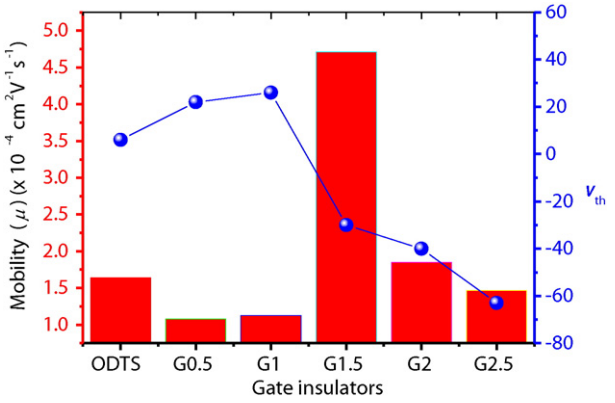

Fig. 6. Effects of gate insulators on the performance of OTFTs based on PDI-C_4F_7.

[9] V. Coropceanu, J. Cornil, D.A. da Silva Filho, Y. Olivier, R. Silbey, J.L. Brédas, Charge transport in organic semiconductors, Chem. Rev. 107 (2007) 926–952.
[10] F.C. Chen, C.H. Liao, Improved air stability of n-channel organic thin-film transistors with surface modification on gate dielectrics, Appl. Phys. Lett. 93 (2008) 103310.
[11] H.C. Tiao, Y.J. Lee, Y.S. Liu, S.H. Lee, C.H. Li, M.Y. Kuo, Effect of hydroxyl density on condensation behaviors of self-assembled monolayers and performance of pentacene-base organic thin-film transistors, Org. Electron. 13 (2012) 1004–1011.
[12] V. Pecunia, K. Banger, H. Sirringhaus, High-performance solution-processed amorphous-oxide-semiconductor TFTs with organic polymeric gate dielectrics, Adv. Electron. Mater. 1 (2015) 1400024.
[13] J.W. Jo, J. Kim, K.T. Kim, J.G. Kang, M.G. Kim, K.H. Kim, H. Ko, Y.H. Kim, S.K. Park, Highly stable and imperceptible electronics utilizing photoactivated heterogeneous sol-gel metal-oxide dielectrics and semiconductors, Adv. Mater. 27 (2015) 1182–1188.
[14] X. Zhao, Q. Zhang, G. Xia, S. Wang, J. Ouyang, J. Zhou, Enhanced performances of organic thin film transistors by dual interfacial modification of dielectric layer, Appl. Phys. A Mater. Sci. Process. 118 (2015) 809–815.
[15] S.A. DiBenedetto, A. Facchetti, M.A. Ratner, T.J. Marks, Molecular self-assembled monolayers and multilayers for organic and unconventional inorganic thin-film transistor applications, Adv. Mater. 21 (2009) 1407–1433.
[16] M.H. Yoon, H. Yan, A. Facchetti, T.J. Marks, Low-voltage organic field-effect transistors and inverters enabled by ultrathin cross-linked polymers as gate dielectrics, J. Am. Chem. Soc. 127 (2005) 10388–10395.
[17] M.A. Rahman, H. Kim, Y.K. Lee, C. Lee, H. Nam, J.S. Lee, H. Soh, J.K. Lee, E.G. Lee, J. Lee, High performance flexible organic thin film transistors (OTFTs) with octadecyltrichlorsilane/Al_2O_3/poly(4-vinylphenol) multilayer insulators, J. Nanosci. Nanotechnol. 12 (2012) 1348–1352.
[18] C.G. Choi, B.S. Bae, Organic–inorganic hybrid gate dielectrics for low-voltage pentacene organic thin film transistors, Synth. Met. 159 (2009) 1288–1291.
[19] C.H. Wang, C.Y. Hsieh, J.C. Hwang, Flexible organic thin-film transistors with silk fibroin as the gate dielectric, Adv. Mater. 23 (2011) 1630–1634.
[20] C.Y. Hsieh, J.C. Hwang, T.H. Chang, J.Y. Li, S.H. Chen, L.K. Mao, L.S. Tsai, Y.L. Chueh, P.C. Lyu, S.S.H. Hsu, Enhanced mobility of organic thin film transistors by water absorption of collagen hydrolysate gate dielectric, Appl. Phys. Lett. 103 (2013) 023303.
[21] S.M. Shau, C.C. Chang, C.H. Lo, Y.C. Chen, T.Y. Juang, S.A. Dai, R.H. Lee, R.J. Jeng, Organic/metallic nanohybrids based on amphiphilic dumbbell-shaped dendrimers, ACS Appl. Mater. Interfaces 4 (2012) 1897–1908.
[22] Y.C. Chen, Y.J. Yang, T.Y. Juang, L.H. Chan, S.A. Dai, F.M. Chen, W.C. Su, R.J. Jeng, Dendronized organic–inorganic nonlinear optical hybrid materials with homogeneous morphology, Synth. Met. 159 (2009) 1852–1858.
[23] Y.C. Chen, T.Y. Juang, T.M. Wu, S.A. Dai, W.J. Kuo, Y.L. Liu, F.M. Chen, R.J. Jeng, Orderly arranged NLO materials based on chromophore-containing dendrons on exfoliated layered templates, ACS Appl. Mater. Interfaces 1 (2009) 2371–2381.
[24] Y.C. Chen, T.Y. Juang, S.A. Dai, T.M. Wu, J.J. Lin, R.J. Jeng, Optical non-linearity from montmorillonite intercalated with a chromophore-containing dendritic structure: a self-assembly approach, Macromol. Rapid Commun. 29 (2008) 587–592.
[25] Y.Y. Siao, S.M. Shau, W.H. Tsai, Y.C. Chen, T.H. Wu, J.J. Lin, T.M. Wu, R.H. Lee, R.J. Jeng, Orderly arranged NLO materials on exfoliated layered templates based on dendrons with alternating moieties at the periphery, Polym. Chem. 4 (2013) 2747.
[26] H.L. Chang, T.Y. Chao, C.C. Yang, S.A. Dai, R.J. Jeng, Second-order nonlinear optical hyperbranched polymers via facile ring-opening addition reaction of azetidine-2,4-dione, Eur. Polym. J. 43 (2007) 3988–3996.
[27] C.H. Wu, S.M. Shau, S.C. Liu, S.A. Dai, S.C. Chen, R.H. Lee, C.F. Hsieh, R.J. Jeng, Enhanced shape memory performance of polyurethanes via the incorporation of organic or inorganic networks, RSC Adv. 5 (2015) 16897–16910.
[28] C.C. Tsai, C.C. Chang, C.S. Yu, S.A. Dai, T.M. Wu, W.C. Su, C.N. Chen, F.M. Chen, R.J. Jeng, Side chain dendritic polyurethanes with shape-memory effect, J. Mater. Chem. 19 (2009) 8484–8494.
[29] C.C. Chang, T.Y. Juang, W.H. Ting, M.S. Lin, C.M. Yeh, S.A. Dai, S.Y. Suen, Y.L. Liu, R.J. Jeng, Using a breath-figure method to self-organize honeycomb-like polymeric films from dendritic side-chain polymers, Mater. Chem. Phys. 128 (2011) 157–165.
[30] Y.A. Su, W.F. Chen, T.Y. Juang, W.H. Ting, T.Y. Liu, C.F. Hsieh, S.A. Dai, R.J. Jeng, Honeycomb-like polymeric films from dendritic polymers presenting reactive pendent moieties, Polymer 55 (2014) 1481–1490.
[31] C.C. Tsai, T.Y. Juang, S.A. Dai, T.M. Wu, W.C. Su, Y.L. Liu, R.J. Jeng, Synthesis and montmorillonite-intercalated behavior of dendritic surfactants, J. Mater. Chem. 16 (2006) 2056–2063.
[32] T.Y. Juang, C.C. Tsai, T.M. Wu, S.A. Dai, C.P. Chen, J.J. Lin, Y.L. Liu, R.J. Jeng, Organo-clay hybrids based on dendritic molecules: preparation and characterization, Nanotechnology 18 (2007) 205606.
[33] J. Mecinovic, P.W. Snyder, K.A. Mirica, S. Bai, E.T. Mack, R.L. Kwant, D.T. Moustakas, A. Heroux, G.M. Whitesides, Fluoroalkyl and alkyl chains have similar hydrophobicities in binding to the "hydrophobic wall" of carbonic anhydrase, J. Am. Chem. Soc. 133 (2011) 14017–14026.
[34] Y. Geng, Q. Wei, K. Hashimoto, K. Tajima, Dipole layer formation by surface segregation of regioregular poly(3-alkylthiophene) with alternating alkyl/semifluoroalkyl side chains, Chem. Mater. 23 (2011) 4257–4263.
[35] C.P. Chen, S.A. Dai, H.L. Chang, W.C. Su, R.J. Jeng, Facile approach to polyurea/malonamide dendrons via a selective ring-opening addition reaction of azetidine-2,4-dione, J. Polym. Sci. A Polym. Chem. 43 (2005) 682–688.
[36] S.A. Dai, T.Y. Juang, C.P. Chen, H.Y. Chang, W.J. Kuo, W.C. Su, R.J. Jeng, Synthesis of N-aryl azetidine-2,4-diones and polymalonamides prepared from selective ring-opening reactions, J. Appl. Polym. Sci. 103 (2007) 3591–3599.
[37] T. Umeda, D. Kumaki, S. Tokito, High air stability of threshold voltage on gate bias stress in pentacene TFTs with a hydroxyl-free and amorphous fluoropolymer as gate insulators, Org. Electron. 9 (2008) 545–549.
[38] S.K. Possanner, P. Pacher, E. Zojer, F. Schürrer, Threshold voltage shifts in organic thin-film transistors due to self-assembled monolayers at the dielectric surface, Adv. Funct. Mater. 19 (2009) 958–967.
[39] K.P. Pernstich, S. Haas, D. Oberhoff, C. Goldmann, D.J. Gundlach, B. Batlogg, A.N. Rashid, G. Schitter, Threshold voltage shift in organic field effect transistors by dipole monolayers on the gate insulator, J. Appl. Phys. 96 (2004) 6431–6438.
[40] M. Marchl, M. Edler, A. Haase, A. Fian, G. Trimmel, T. Griesser, B. Stadlober, E. Zojer, Tuning the threshold voltage in organic thin-film transistors by local channel doping using photoreactive interfacial layers, Adv. Mater. 22 (2010) 5361–5365.

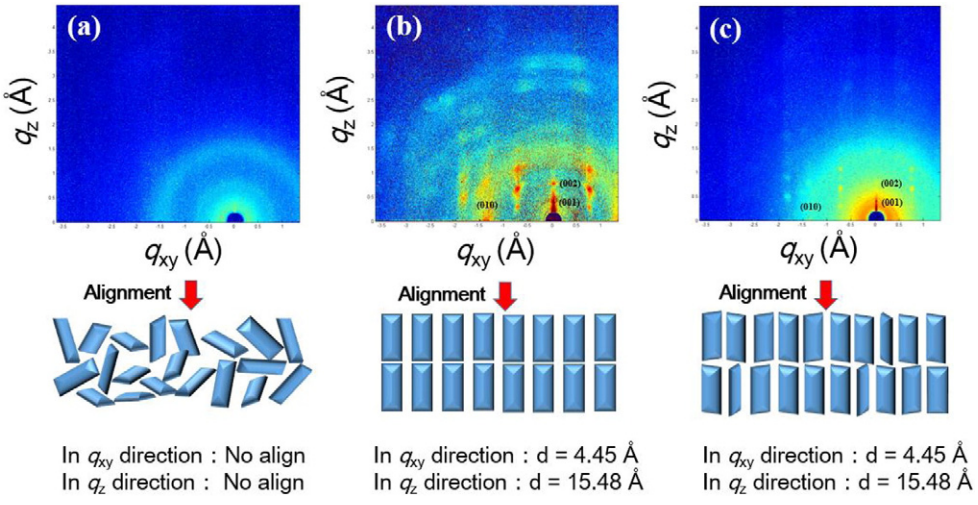

Fig. 7. 2-D GIWAXS patterns of PDI-C_4F_7 on dendron gate insulators: (a) G0.5, (b) G1.5, (c) G2.5.

[41] M. Aghamohammadi, R. Rödel, U. Zschieschang, C. Ocal, H. Boschker, R.T. Weitz, E. Barrena, H. Klauk, Threshold-voltage shifts in organic transistors due to self-assembled monolayers at the dielectric: evidence for electronic coupling and dipolar effects, ACS Appl. Mater. Interfaces 7 (2015) 22775–22785.
[42] J. Jang, S. Nam, D.S. Chung, S.H. Kim, W.M. Yun, C.E. Park, High Tg cyclic olefin copolymer gate dielectrics for N,N′-ditridecyl perylene diimide based field-effect transistors: improving performance and stability with thermal treatment, Adv. Funct. Mater. 20 (2010) 2611–2618.
[43] F. Zhang, Y. Hu, T. Schuettfort, C.A. Di, X. Gao, C.R. McNeill, L. Thomsen, S.C. Mannsfeld, W. Yuan, H. Sirringhaus, D. Zhu, Critical role of alkyl chain branching of organic semiconductors in enabling solution-processed N-channel organic thin-film transistors with mobility of up to 3.50 $cm^2 V^{-1} s^{-1}$, J. Am. Chem. Soc. 135 (2013) 2338–2349.
[44] S.D. Wang, T. Miyadera, T. Minari, Y. Aoyagi, K. Tsukagoshi, Correlation between grain size and device parameters in pentacene thin film transistors, Appl. Phys. Lett. 93 (2008) 043311.
[45] Y. Hu, Q. Qi, C. Jiang, Influence of different dielectrics on the first layer grain sizes and its effect on the mobility of pentacene-based thin-film transistors, Appl. Phys. Lett. 96 (2010) 133311.
[46] R.J. Chesterfield, J.C. McKeen, C.R. Newman, P.C. Wbank, D.T.A. da Silva Filho, J.L. Bre'das, L.L. Miller, K.R. Mann, C.D. Frisbie, Organic thin film transistors based on N-alkyl perylene diimides: charge transport kinetics as a function of gate voltage and temperature, J. Phys. Chem. B 108 (2004) 19281–19292.
[47] L. Hao, C. Xiao, J. Zhang, W. Jiang, Y.W. Xu, Z. Wang, Perpendicularly entangled perylene diimides for high performance electron transport materials, J. Mater. Chem. C 1 (2013) 7812–7818.